High contrast ratio, high uniformity multiple quantum well spatial light modulators

Yuyang, Huang; Liu, H. C.; Wasilewski, Z. R.; Buchanan, M.; Laframboise, S. R.; Yang, Chen; Cui, Guoxin; Bian, Lifeng; Yang, Hui; Yaohui, Zhang

Publisher's version / Version de l'éditeur:
https://doi.org/10.1088/1674-4926/31/3/034007
Journal of Semiconductors, 31, 3, pp. 1-4, 2010-03-01

High contrast ratio, high uniformity multiple quantum well spatial light modulators*

Huang Yuyang(黄寓洋)[1,2], Liu H C(刘惠春)[2,3], Wasilewski Z R[3], Buchanan M[3], Laframboise S R[3], Yang Chen(杨晨)[1,2], Cui Guoxin(崔国新)[2], Bian Lifeng(边历峰)[2], Yang Hui(杨辉)[1,2], and Zhang Yaohui(张耀辉)[2,†]

(1 Institute of Semiconductors, Chinese Academy of Sciences, Beijing 100083, China)
(2 Suzhou Institute of Nano-Tech and Nano-Bionics, Chinese Academy of Sciences, Suzhou 215125, China)
(3 Institute for Microstructural Sciences, National Research Council, Ottawa K1A 0R6, Canada)

Abstract: Our latest research results on GaAs–AlGaAs multiple quantum well spatial light modulators are presented. The thickness uniformity of the epitaxial layers across the 3-inch wafer grown by our molecular beam epitaxy is better than 0.1% and the variation of cavity resonance wavelength within the wafer is only 0.9 nm. A contrast ratio (CR) of 102 by varying bias voltage from 0 to 6.7 V is achieved after fine tuning the cavity by etching an adjust layer. Both theoretical and experimental results demonstrate that incorporating an adjust layer is an effective tuning method for obtaining high CR.

Key words: spatial light modulator; multiple quantum well; uniformity; contrast ratio; adjust layer; matching condition
DOI: 10.1088/1674-4926/31/3/034007 **PACC:** 4280K; 4265P

1. Introduction

The quantum-confined Stark effect (QCSE), reported by Miller *et al.* in 1984[1], had been used in multiple quantum well (MQW) electroabsorption modulators in the late 1980s. Later, the Fabry–Perot (F–P) cavity was introduced[2,3], which made high contrast ratio (CR), low drive voltage and low insertion loss modulators realizable. Nowadays, the spatial light modulator (SLM) has become a key component in many electro-optic applications, for example, optical computation[4], free-space optical communication[5], optical correlation[6] and laser beam steering[7]. High CR, low driving voltage, low insertion loss SLMs have been reported[8]. To our knowledge, the best CR and uniformity reported in mainland of China are about $10:1$[9] and 2.2%[10]. In our latest research development, uniformity of better than 0.1% and CR of 102 are achieved.

The most common structure of MQW SLM is to embed i-type MQW absorption area between p- and n-type distributed Bragg reflector (DBR) mirrors, which form an asymmetric F–P cavity with absorption[3]. In this structure, MQW introduces enhanced absorption peak at the heavy hole exciton resonance wavelength (λ_{EX}), while the F–P cavity provides resonance reflection at a certain wavelength (λ_{FP}), which is also the working wavelength of the device. λ_{FP} is usually placed at the longer wavelength side of λ_{EX}. The operation principle is to move λ_{EX} toward λ_{FP} by applying an electric field (according to QCSE) in order to lead a change in both absorption and reflectivity at λ_{FP}.

The performance of the modulator is primarily characterized by its CR，the ratio between the amount of light reflected in the ON state (R_{ON}) and in the OFF state (R_{OFF}). Near-zero R_{OFF} is important for a high CR. A matching condition (balance condition) which must be satisfied to achieve a near-zero R_{OFF}[11] is as follows:

$$R_f = R_b \exp(-2\alpha L) = R_{beff}, \tag{1}$$

where R_f, R_b is the reflectivity of front and back mirror, α is the absorption coefficient in MQW, L is the length of F–P cavity, and R_{beff} is the effective reflectivity of back mirror.

2. Material design, growth and device fabrication

Computer modeling and calculation are used for material design[12,13]. After that, the multi-layer structure (labeled V0726) is grown in a V90 molecular beam epitaxy (MBE) system on a GaAs wafer. The schematic diagram of the material is shown in Fig. 1. In the direction from the top epitaxial layer to the substrate, there are 1000 Å $Al_{0.2}Ga_{0.8}As$ adjust layer, 5 periods of n-type front DBR, 28 periods of 72 Å/45 Å GaAs/$Al_{0.35}Ga_{0.65}As$ MQW, n-contact GaAs layer, 25 periods of p-type bottom DBR, and etching stop layer. Because the only one Al source in the MBE system is calibrated for $Al_{0.5}Ga_{0.5}As$ (not $Al_{0.1}Ga_{0.9}As$) at the time of this growth, short period superlattice (GaAs (40 Å)/$Al_{0.5}Ga_{0.5}As$ (10 Å)) is used to serve as a layer of $Al_{0.1}Ga_{0.9}As$ to obtain a high accuracy of growth rate and Al concentration. The wafer is rotated during the MBE growth to ensure a good uniformity. λ_{EX} and λ_{FP} are designed at 840 nm and 860 nm, respectively.

Single pixel devices were fabricated by a three-step process: top ring p-contact deposition and lift-off, mesa wet-etching and bottom n-contact deposition and lift-off. Mesa devices were then packaged and wire-bonded for measurement.

* Project supported by the President Fund of CAS, the International Collaboration Plan for Science and Technology of the Chinese Ministry of Science and Technology (No. 2008KR0415), and the Suzhou International Cooperation Fund, China (No. SWH0809).
† Corresponding author. Email: yhzhang2006@sinano.ac.cn
Received 7 September 2009, revised manuscript received 20 December 2009

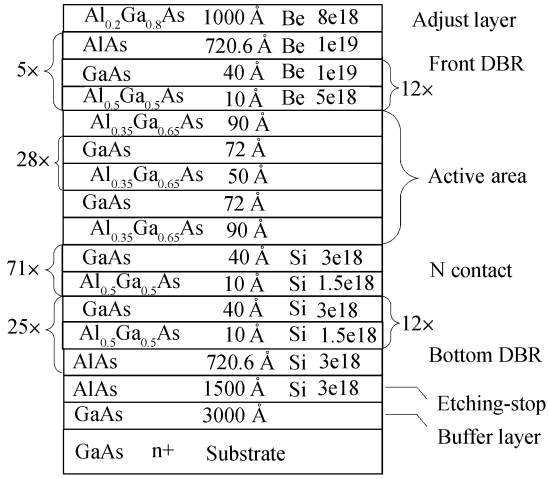

Fig. 1. Multi-layer structure of V0726.

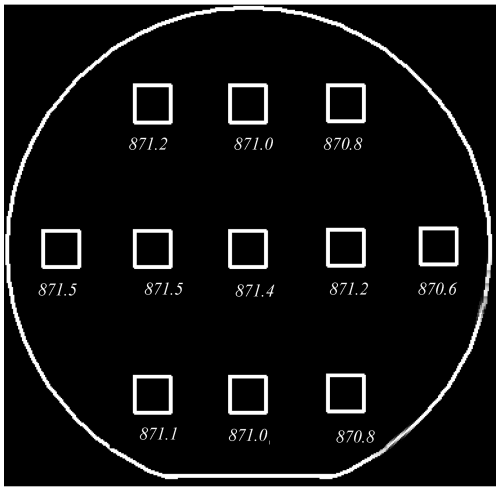

Fig. 2. Measured F–P mode (λ_{FP}) position across the whole wafer (nm). Maximum variation of λ_{FP} is only 0.9 nm.

The mesa size of the device is from 400×400 μm^2 to 4000×4000 μm^2.

3. Experiment results

First, we measured the reflectivity spectra of the material to evaluate its optical properties using a Fourier transform infrared spectroscopy (FTIR) system. The light source is collimated and focused to 0.5 mm diameter. Only the center of the reflected beam is collected to ensure good direction consistency. The test results show λ_{EX} is at 836 nm, while λ_{FP} is at 871 nm. The deviation between designed and measured values is caused by a slightly larger than intended MBE growth rate. This growth rate error can be estimated by the deviation of λ_{FP}: (871 – 860)/860 = +1.3%. Indeed, an X-ray diffraction (XRD) analysis shows that the layer thickness is about 1% larger than the designed value. If we re-model the device performance with the new parameters extracted from XRD, λ_{FP} should be at 873 nm, very close to the experimental data. This confirms the validity of our modeling and design. Greater accuracy for layer thickness, thus even more accurate mode location, can be achieved with MBE reproducibly, but only by employing *in-situ* growth rate monitoring coupled real-time to the recipe execution.

The lateral uniformity is important for the development of a high volume 2-D SLM array. We picked 11 points across the whole wafer to evaluate the uniformity. The λ_{FP} position mapping is shown in Fig. 2. The maximum variation of λ_{FP} across the wafer diameter is 0.9 nm. The lateral uniformity of the device structure is within $0.9/871 = 0.1\%$[14]. This has been achieved by optimizing the geometry of the MBE system and of the molecular beams. Previous reports on this value is 0.7% across a 4-inch wafer[15]. To our knowledge, our result is the best for this kind of device to date.

Under normal incidence conditions, the measured wavelength spacing between λ_{EX} and λ_{FP} is 35 nm, which is too large to get a high absorption change for a high CR. (The proper spacing between λ_{EX} and λ_{FP} is about 10–15 nm.). In this case, a very high drive voltage is required. To solve this problem, an oblique incident angle is utilized to decrease the spacing. Under the 40-degree incident angle condition, λ_{FP} is shifted from 871 to 860 nm and CR of 14 is achieved. However, even in such a large incident angle, there is still a 24 nm spacing between λ_{EX} and λ_{FP}. When λ_{EX} is shifted into λ_{FP} by such a long distance, the exciton absorption at this point will be too weak to fulfill the matching condition. A top adjust layer is adopted to overcome the problem. (The principles of adjust layer will be discussed in the next section.) The 400-Å-thick adjust layer on the top is wet-etched and the reflectivity spectra are re-measured. After the adjustment, λ_{FP} is shifted by 4 nm to the shorter wavelength side and the near-zero reflectivity is achieved at 6.7 V with CR = 102. The reflectivity spectra before and after adjust layer etching are shown in Fig. 3.

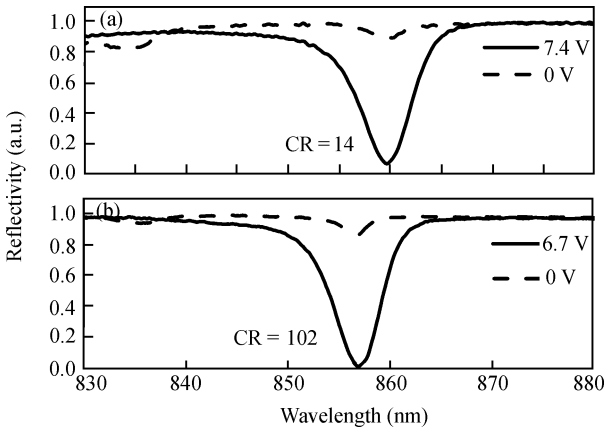

Fig. 3. Measured reflectivity spectra (a) before and (b) after 400-Å adjust layer etching.

4. Discussion

In the design and fabrication process of MQW SLMs, the allocation of λ_{EX} and λ_{FP} is very important. Their positions determine the working wavelength, while the spacing between them dictates the modulation depth and CR value. However, λ_{FP} is very sensitive to the layer thickness of the epitaxial material. Generally, a small deviation of the experimental result from the designed value exists, unless the growth rate is strictly calibrated and *in-situ* correction is introduced during

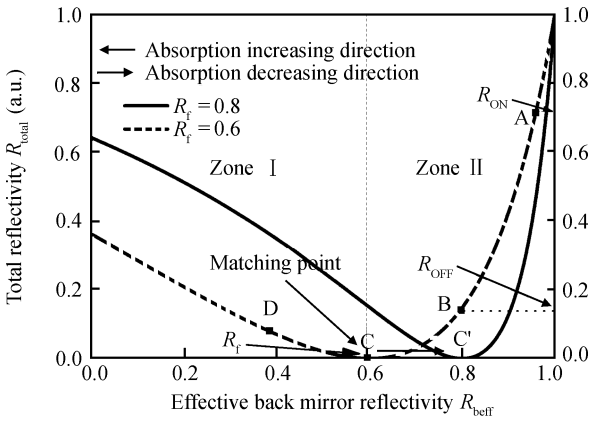

Fig. 4. Total reflectivity versus effective bottom mirror reflectivity with given $R_f = 0.6$ and 0.8. R_{beff} is inversely proportional to α, so from left to right (R_{beff} increasing) means α decreasing, from right to left means α increasing.

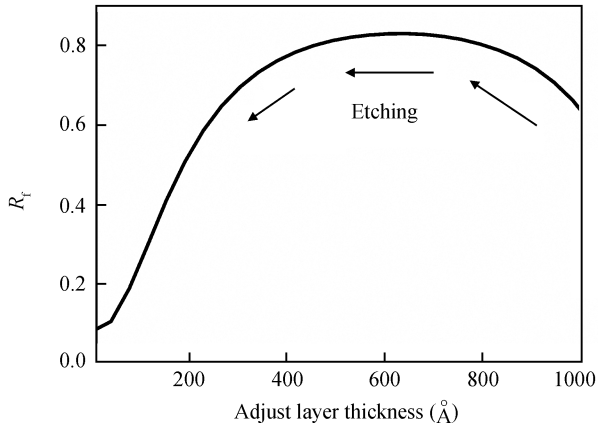

Fig. 5. Calculated R_f versus adjust layer thickness.

the growth process[16]. When the spacing between λ_{EX} and λ_{FP} is larger or smaller than the designed value, the absorption coefficient at working wavelength can be changed substantially because of the intensity change of QCSE effect under applied electric field. Adjust layer etching is a practical way to solve the problem. This method has been reported before[17], but unlike the previous paper, here we will focus on the effect of the matching condition tuning.

Equation (2) describes the relationship between the device total reflectivity (R_{total}) and R_{beff} for a given R_f at λ_{FP}[18]:

$$R_{total} = \left| \frac{R_f - R_{beff}}{1 - R_f R_{beff}} \right|^2 . \quad (2)$$

The calculated relationship is shown in Fig. 4. See dashed line curve for $R_f = 0.6$. Under zero electrical field, the absorption at F–P mode is small and R_{beff} is large. At this moment the device works at zone II, hypothetically at point A. With a small biased voltage, the absorption coefficient increases, making R_{beff} decrease. Thus, the working point moves left along the curve to B. When R_{beff} decreases to R_f, the working point shifts to point C and a near-zero R_{OFF} is achieved. Point C, whose horizontal coordinate equals to R_f, is usually called the matching point. However, in our experiment, the spacing between λ_{EX} and λ_{FP} is large and the absorption at λ_{FP} is very small with biased voltage. In Fig. 4, it means the working point is just near B, unable to reach the matching point C. If we can find a method to adjust the position of point C (as well as R_f), it is possible to satisfy the matching condition.

As an additional layer above top DBR, the 1000-Å $Al_{0.2}Ga_{0.8}As$ adjust layer is used to make a change of R_f. We calculate R_f versus adjust layer thickness using transform matrix method[19], which is shown in Fig. 5. By etching the adjust layer, R_f increases from 60% to 80%, then decreases to 10%. In Fig. 4, this means we can adjust the matching point (C) position in a very wide range. If the adjust layer is etched by about 400 Å, R_f will increase from 60% to 80% and the solid curve will become the new working line. The working point of device will be changed from B to C', so a lower low-state reflectivity can be realized. Moreover, an etching of the adjust layer will shift the F–P mode to the short-wavelength side, making the absorption at F–P position larger and the matching condition easier to satisfy. Experimental data (Fig. 3) shows clearly that by such an adjustment method, R_{OFF} decreases from 6.3% to 0.8% and CR increases from 14 to 102, and λ_{FP} is blue-shifted by about 4 nm, which is in accordance with the theory[17].

5. Conclusion

We have presented our latest research results on MQW SLMs in this paper. The material is grown by MBE. A spread of only 0.9 nm of λ_{FP} is achieved across the 3-inch-diameter wafer, representing a lateral uniformity of better than 0.1%. The single pixel devices are fabricated and the reflectivity spectra are measured. When the incident angle is 40 degree, CR reaches 14 for the applied bias voltage of 7.4 V. After etching the adjust layer which is on the top of the device to tune the matching condition, CR is successfully increased to 102 at 6.7 V voltage. This work is an indispensable base toward the fabrication of 2-D arrays of GaAs/AlGaAs MQW SLM bonded to CMOS driving circuit in the following research.

Acknowledgement

One of us (Huang Yuyang) thanks Richard Dudek for device assembling during his stay at the Institute for Microstructural Sciences, National Research Council, Canada.

References

[1] Miller D A B, Chemla D S, Damen T C, et al. Band-edge electroabsorption in quantum well structures: the quantum-confined Stark effect. Phys Rev Lett,1984, 53(22): 2173
[2] Boyd G D, Miller D A B, Chemla D S, et al. Multiple quantum well reflection modulator. Appl Phys Lett, 1987, 50(17): 1119
[3] Whitehead M, Parry G. High-contrast reflection modulation at normal incidence in asymmetric multiple quantum well Fabry-Perot structure. Electron Lett, 1989, 25(9): 566
[4] Efron U. Spatial light modulators for optical computing. Proc SPIE,1986, 700: 132
[5] Gilbreath G, Rabinovich W, Meehan T, et al. Large-aperture multiple quantum well modulating retroreflector for free-space optical data transfer on unmanned aerial vehicles. Opt Eng, 2001, 40: 1348
[6] Kang K, Powell J S, Stack R D, et al. Optical image correlation using high-speed multiple quantum well spatial light modulators. Proc IEEE, 1999, 3715: 97

[7] Ahearn J, Weiler M, Adams S, et al. Multiple quantum well (MQW) spatial light modulators (SLMs) for optical data processing and beam steering. SPIE Conference, 2001: 43
[8] Wang Q, Junique S, Agren D, et al. Arrays of vertical-cavity electroabsorption modulators for parallel signal processing. Opt Express, 2005, 13(9): 3323
[9] Chen Hongda, Chen Zhibiao, Du Yun, et al. Exciton absorption and modulating characters in multiple quantum well switches. Journal of Optoelectronics·Laser, 2000, 11(2): 143 (in Chinese)
[10] Wu R H, Chen Z B, Chen H D, et al. 8×8 multiple quantum well spatial light modulators for optical interconnection. Chinese Journal of Lasers, 1998, 25(7): 603 (in Chinese)
[11] Yan R H, Simes R J, Coldren L A. Surface-normal electroabsorption reflection modulators using asymmetric Fabry–Perot structures. IEEE J Quantum Electron, 1991, 27(7): 1922
[12] Stevens P J, Whitehead M, Parry G, et al. Computer modeling of the electric field dependent absorption spectrum of multiple quantum well material. IEEE J Quantum Electron, 1988, 24(10): 2007
[13] Nakamura K, Shimizu A, Fujii K, et al. Numerical analysis of the absorption and the refractive indexchange in arbitrary semiconductor quantum-well structures. IEEE J Quantum Electron, 1992, 28(7): 1670
[14] Zouganeli P, Parry G. Evaluation of the tolerance of asymmetric Fabry–Perot modulators with respect to realistic operating conditions. IEEE J Quantum Electron, 1995, 31(6): 1140
[15] Arad U, Redmard E, Shamay M, et al. Development of a large high-performance 2-D array of GaAs-AlGaAs multiple quantum-well modulators. IEEE Photonics Technol Lett, 2003, 15(11): 1531
[16] Bacher K, Pezeshki B, Lord S M, et al. Molecular beam epitaxy growth of vertical cavity optical devices with in situ corrections. Appl Phys Lett, 1992, 61(12): 1387
[17] Wu Ronghan, Chen Zhibiao, Chen Hongda, et al. Mode adjustment in multiple quantum well asymmetric Fabry–Perot modulator. Chinese Journal of Semiconductors, 1998, 19(5): 341 (in Chinese)
[18] Trezza J A, Harris J J S. Creation and optimization of vertical cavity phase flip modulators. J Appl Phys, 1994, 75(10): 4878
[19] Yeh P. Optical waves in layered media. New York: Wiley, 1988